Phys. Status Solidi A **210,** No. 7, 1424–1428 (2013) / **DOI** 10.1002/pssa.201228682

physica status solidi a
www.pss-a.com
applications and materials science

Nanoscale light guiding in a silicon-based hybrid plasmonic waveguide that incorporates an inverse metal ridge

Yusheng Bian[1], Zheng Zheng[*,1], Xin Zhao[1], Lei Liu[1], Yalin Su[1], Jiansheng Liu[1], Jinsong Zhu[2], and Tao Zhou[3]

[1] School of Electronic and Information Engineering, Beihang University, 37 Xueyuan Rd, Beijing 100191, P. R. China
[2] National Center for Nanoscience and Technology, No.11 Zhongguancun Beiyitiao, Beijing 100190, P. R. China
[3] Department of Physics, New Jersey Institute of Technology, Newark, NJ 07102, USA

Received 7 October 2012, revised 27 February 2013, accepted 5 March 2013
Published online 5 April 2013

Keywords integrated photonics, silicon, surface plasmons, waveguides

[*] Corresponding author: e-mail zhengzheng@buaa.edu.cn, Phone: 086-010-82317220, Fax: 086-010-82317220

A silicon-based hybrid plasmonic waveguide that comprises an inverse metal ridge sitting above a silicon-on-insulator substrate with a nanometre-thick, low-index gap is proposed and its guiding mode properties are analyzed numerically at the wavelength of 1,550 nm. The strongly hybridized modes supported by the inverse metal ridge and the thin silicon layer provide an efficient scheme to store the optical field inside the nanoscale gap region with strong local field enhancement. Compared to the previously studied hybrid plasmonic waveguides based on the coupling between metal wedges or metal ridges with finite-wide high-index nanowires, the present hybrid waveguide leveraging inverse metallic wedge with infinite-wide silicon layer simplifies the fabrication process to a certain extent and avoids the lateral misalignment that is rather challenging to control in many other hybrid plasmonic wave-guiding counterparts. Besides, the studied structure also shows the potential to further reduce the mode size of conventional hybrid waveguide based on flat metal substrate, thus making itself an attractive building block for compact photonic integrated components and circuits.

1 Introduction Nanoscale confinement of light has drawn increasing attention recently, due to its prospect of enabling extensive investigations on extremely light–matter interactions far beyond the diffraction limit [1]. A number of guiding schemes had been proposed and demonstrated to achieve the goal of tight field confinement. Among them, photonic crystal fibers [2] and silicon nanowire waveguides [3] exhibit the capability of confining light at the wavelength scale, while silicon slot waveguides could offer the potential for subwavelength guiding along one direction [4]. Truly nanoscale light confinement in two directions can be enabled by structures involving surface plasmons (SPs) [5, 6]. Due to the strong light–matter interactions, the length of photonic devices leveraging plasmonic structures can be much shorter than that of the conventional pure dielectric components, thus greatly facilitating the miniaturization of photonic integrated circuits [7]. However, due to the large overlap of optical field with dissipative metallic waveguides, the propagation loss of plasmonic structures is relatively large.

In order to simultaneously realize low modal loss and strong optical confinement, a novel guiding scheme that enables light transport inside a small gap between high-index semiconductor nanostructure and metallic plane has been presented recently [8, 9]. Owing to the strong interaction between dielectric and plasmonic modes, the hybrid system is able to reduce the propagation loss greatly with an ultra-tight mode confinement. Along with other attractive features such as low-crosstalk and broadband operation, the hybrid waveguides can be utilized as important building blocks in highly integrated photonic circuits [10, 11]. Besides the demonstration of various compact photonic components leveraging hybrid structures [12–16], a number of modified waveguides with novel optical properties have also been studied [7, 17–21]. It is revealed that by employing metal wedge or ridge substrate instead of the flat metallic surface, the confinement capability can be further improved while remaining low-modal-loss [18–20]. However, despite the enhanced optical performance, these presented structures

are more challenging to realize than the conventional hybrid waveguide. Additional fabrication complexity and/or alignment errors set a limitation to their practical implementations. Here in this paper, we propose an alternative hybrid waveguide that consists of an inverse metal ridge sitting above a thin silicon layer with infinite width. Besides providing nanoscale light confinement with low propagation loss, such a hybrid structure also avoids the lateral misalignment between the dielectric and metal surface, which offers great beneficial for its further applications.

2 Modal properties of the inverse metal ridge based hybrid plasmonic waveguide The 3D geometry of the studied hybrid waveguide is schematically shown in Fig. 1, where a trapezoidal/rectangular upside-down silver ridge is separated from a thin silicon layer by a nanoscale silica gap. The top cladding and the substrate are made of silver and silica, respectively, while other regions are assumed to be filled with silica. The bottom and top widths of the ridge are denoted as w_b and w_t. The metal ridge height is h whereas the sidewall angle of the ridge is θ. The thicknesses of the gap and the silicon layer are g and t, respectively. The modal properties of the present waveguide are investigated at $\lambda = 1{,}550$ nm using the finite-element method (FEM) based software COMSOL^{TM}. Scattering boundary conditions along with extremely fine mesh are applied to ensure accurate solutions. The permittivities of silicon, silica and silver are $\varepsilon_d = 12.25$, $\varepsilon_s = \varepsilon_c = 2.25$ and $\varepsilon_m = -129 + 3.3i$ [8], respectively.

Here we look into the fundamental quasi-TM hybrid plasmonic mode that is capable of squeezing a relatively large portion of the optical field inside the nanoscale gap between the inverse metal ridge and the silicon layer. The electric field distributions of the considered hybrid mode supported by the waveguide are shown in Fig. 2, where the geometrical parameters are chosen as: $w_b = h = 200$ nm, $\theta = 10^\circ$, $t = 100$ nm and $g = 10$ nm. As seen clearly in the 2D field panel, field enhancement occurs inside the low-index silica gap region with reasonable modal overlap with the thin silicon layer, which is also manifested in the corresponding

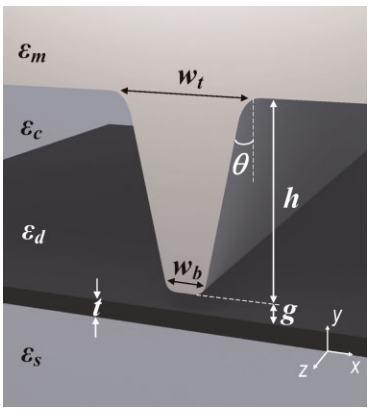

Figure 1 Layout of the proposed inverse metal ridge type hybrid plasmonic waveguide.

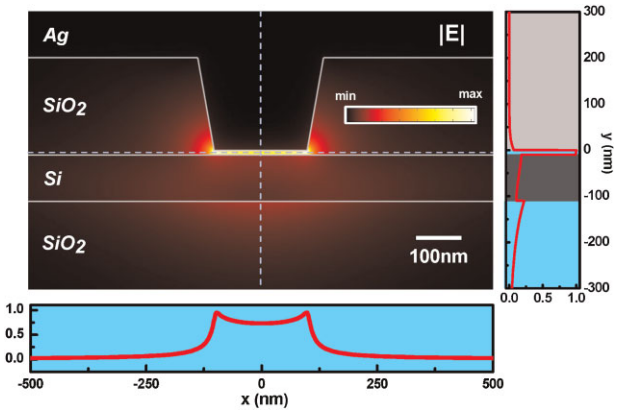

Figure 2 Electric field distributions of the studied fundamental quasi-TM hybrid mode supported by the proposed waveguide ($\theta = 10^\circ$, $w_b = h = 200$ nm, $t = 100$ nm, $g = 10$ nm). Field distributions along the dashed lines in the 2D panel illustrate the strong field enhancement in the low-index silica gap between the metal ridge and the silicon layer.

cross-sectional field plots. From the field distribution along the lateral (x) direction, it is also illustrated that the electric fields near the two bottom corners of the metal ridge can be enhanced greatly, due to the excitation of wedge plasmon polaritons [22, 23].

To obtain a comprehensive understanding of the modal properties, we investigate the dependence of optical performances on key geometric parameters of the hybrid waveguide. By fixing the bottom width and height of the metal ridge at 100 and 200 nm, we show the calculated modal properties of the studied mode at different t with a maintained gap thickness of 10 nm. In Fig. 3(a)–(d), n_{eff} is the real part of the complex mode effective index N_{eff}. The propagation distance (L) is obtained by $L = \lambda/[4\pi \mathrm{Im}(N_{eff})]$. The effective mode area is calculated using $A_{eff} = (\iint W(\boldsymbol{r})\mathrm{d}A)^2/(\iint W(\boldsymbol{r})^2\mathrm{d}A)$. In order to accurately account for the energy in the metal region, the electromagnetic energy density $W(\boldsymbol{r})$ is defined as [8]

$$W(\boldsymbol{r}) = \frac{1}{2}\mathrm{Re}\left\{\frac{\mathrm{d}[\omega\varepsilon(\boldsymbol{r})]}{\mathrm{d}\omega}\right\}|E(\boldsymbol{r})|^2 + \frac{1}{2}\mu_0|H(\boldsymbol{r})|^2. \quad (1)$$

In the equation, $E(\boldsymbol{r})$ and $H(\boldsymbol{r})$ are the electric and magnetic fields, $\varepsilon(\boldsymbol{r})$ is the electric permittivity and μ_0 is the vacuum magnetic permeability. A_0 is the diffraction-limited mode area in free space and defined as $\lambda^2/4$. NOP is defined as the ratio of the power inside the considered region to the total power in the overall waveguide. It is shown in Fig. 3a that for all the considered sidewall angles, the mode effective index increases monotonically with the increasing of the silicon layer thickness. On the other hand, the propagation distance, mode area as well as the optical power inside the silica gap exhibit non-monotonic trends. As can be seen from Fig. 3b and c, both L and A_{eff} reach their minimum values when the thickness of the silicon layer is moderate, which corresponds

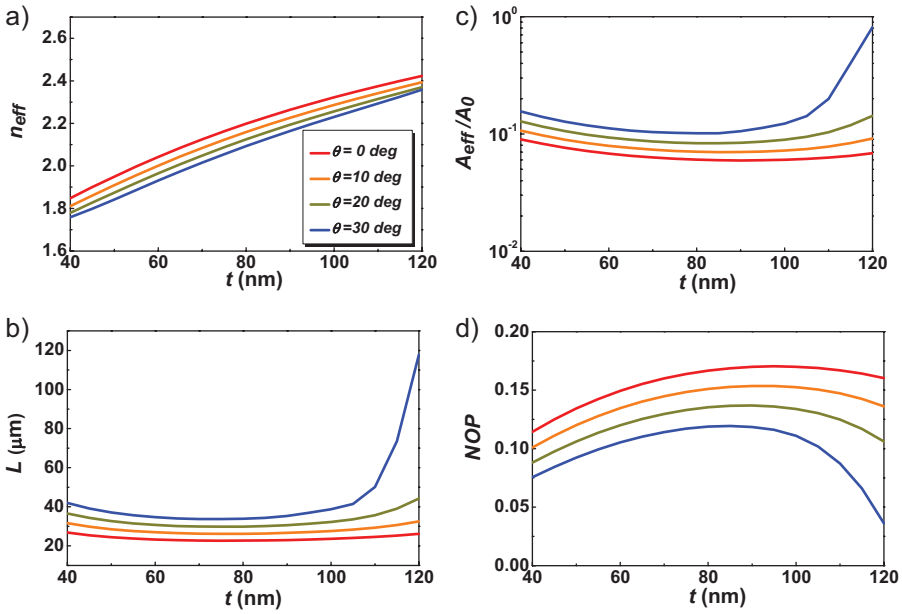

Figure 3 Dependence of modal properties of the studied hybrid plasmonic waveguide on the thickness of the silicon layer: (a) mode effective index (n_{eff}); (b) propagation distance (L); (c) normalized mode area (A_{eff}/A_0); (d) normalized optical power (NOP) in the silica gap.

to the strongest hybridization between the dielectric and plasmonic modes. According to the coupled mode theory, near the strongest coupling conditions, the effective indices of the two modes match each other, which also results in the largest optical power confined inside the silica gap between the metal ridge and the silicon layer. Here, for different sidewall angles, the metal ridge varies and its supported plasmonic mode has a different effective index, which consequently leads to a slightly different critical silicon layer thickness to attain the strongest hybridization between the two modes for each θ. It is also illustrated that, by making the sidewall of the metal wedge less steep (i.e. with larger θ), the propagation distance can be further extended. This provides an additional freedom to reduce the propagation loss of hybrid waveguides besides engineering the gap thickness, as opposed to the conventional hybrid plasmonic structure. Our simulations also indicate that by reducing the height of the metal ridge, the modal behaviour of the proposed waveguide gradually would approach that of the conventional hybrid structure with infinite metal surface, leading to a reduced modal loss and also an increased mode area. When the metal ridge disappears, the whole waveguide turns into a one-dimensional conventional hybrid plasmonic structure, with most of the modal field stored in the thickness-uniform insulator layer between the upper metal cladding and the lower silicon layer.

We further investigate the properties of the considered hybrid mode when the metal ridge width varies, whereas the thicknesses of the gap and silicon layer are fixed at 10 and 100 nm, respectively, with the ridge height maintained at 200 nm. Here, the silicon layer thickness is chosen at a moderate value in order to ensure relatively strong interaction between the dielectric and plasmonic modes. As shown in Fig. 4a and d, the mode effective index and normalized optical power exhibit similar trends with increased ridge width for different sidewall angles. It is illustrated that n_{eff} reaches its maximum at a certain w_b while decreasing slightly when the bottom width exceeds the critical value. In contrast, gradually increased optical power inside the gap can be achieved at larger w_b. This phenomenon is largely due to the increased gap area when the metal ridge gets wider. Such an increasing pace would slow down when the ridge is relatively wide, indicating near-saturated optical power in the gap, as can be seen from the curves in Fig. 4d (e.g. when $w_b > 300$ nm).

On the other hand, the propagation distance and the mode area demonstrate quite different trends against the variation of w_b for different sidewall angles. For large sidewall angle case (e.g. $\theta = 10^\circ$, 20°, 30°), L and A_{eff} decrease first before they increase as the metal ridge becomes wider. By contrast, when θ is small (e.g. $\theta = 0^\circ$ or 5° (not shown)), reduced propagation loss along with increased mode area can be achieved at large w_b. The above phenomena related to different trends of propagation loss and mode area at varied sidewall angles also can be explained by the coupled mode theory. The occurrence of local minimum position of L or A_{eff} at large θ corresponds to the strongest coupling condition, where the effective index of plasmonic mode equals that of the dielectric mode, similar as that shown in Fig. 3. By contrast, when the angle is small, due to the mismatch between the two modes' indices within the chosen parameter range, the coupling strength between them exhibits a monotonic trend, which consequently results in the monotonic behaviour of the propagation loss and the mode area. It is expected that the strongest hybridization condition for $\theta = 0^\circ$ case can be met by further reducing the metal ridge width or adopting thicker silicon layers. Furthermore, it is also illustrated that, similar to the case as studied in Fig. 3, for a fixed w_b, increasing the sidewall angle results in a decreased mode effective index, reduced propagation loss

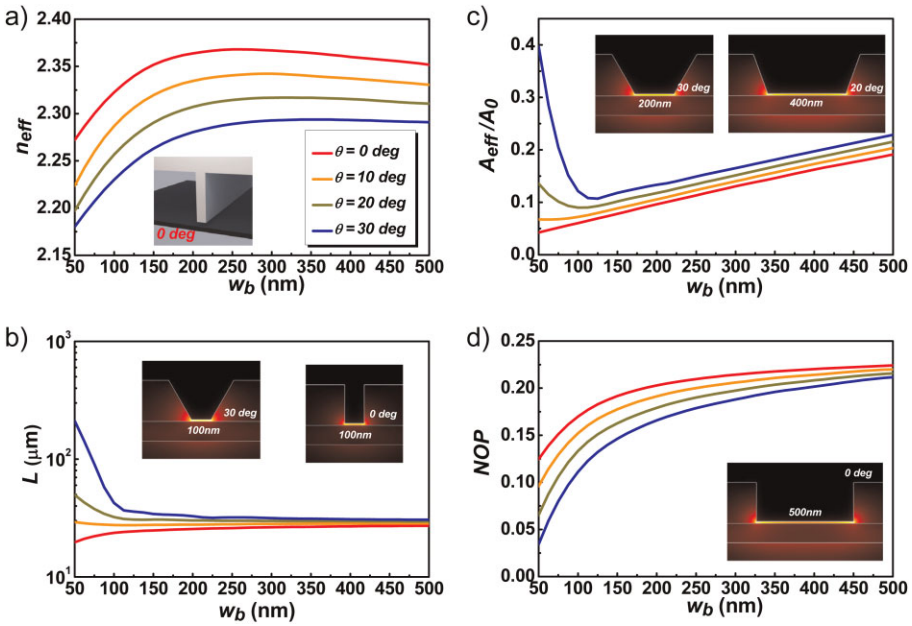

Figure 4 Modal properties of the studied hybrid waveguide: (a) mode effective index (n_{eff}); (b) propagation distance (L); (c) normalized mode area (A_{eff}/A_0); (d) normalized optical power resided in the silica gap (NOP). The inset in (a) shows the geometry of the waveguide with $\theta = 0^\circ$, while the insets in (b–d) demonstrate typical electric field distributions.

and optical power in the gap, as well as an increased effective mode area (see also the insets). Within the considered range of ridge widths, the studied hybrid plasmonic mode is able to simultaneously achieve nanoscale optical confinement and low propagation loss, while ensuring a reasonable portion of the optical power located inside the silica gap. In order to benchmark the properties of the proposed silicon-based hybrid plasmonic waveguide, we further compare its optical performance with the conventional hybrid plasmonic structure having the same gap width. The calculated result is depicted in Fig. 5. It is shown that, for an optimized conventional hybrid plasmonic waveguide consisting of a 200 nm × 200 nm square silicon nanowire sitting above a flat metal substrate with a 10 nm silica gap, the effective mode area is around 0.1. In contrast, the presented hybrid structure is able to achieve an even smaller mode area with the same gap thickness, while still retaining a reasonable propagation distance, as can be seen in Fig. 5. On the other hand, compared to the conventional hybrid waveguide, the proposed structure can achieve much longer propagation distance with subwavelength mode area by choosing larger angles. The unique properties of the present hybrid waveguide offer more flexibility for practical applications and make it an attractive candidate for the realization of compact photonic components.

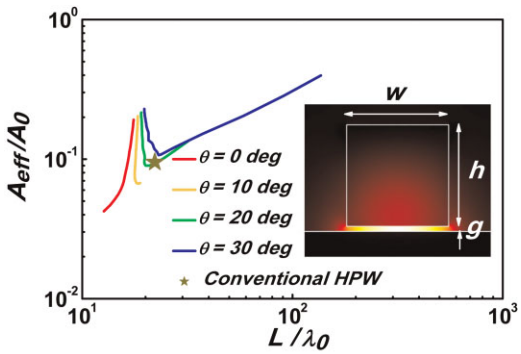

Figure 5 Performance comparison between the proposed silicon based hybrid plasmonic waveguide (w_b: 50–500 nm, $h = 200$ nm, $g = 10$ nm) and the conventional hybrid structure ($w = h = 200$ nm, $g = 10$ nm). The inset shows the electric field distribution of the supported plasmonic mode for the conventional hybrid waveguide.

3 Conclusions In this paper, we have proposed and investigated a novel hybrid plasmonic waveguide that comprises an inverse metal ridge near a thin silicon structure. Numerical simulations reveal that nanoscale light confinement can be enabled with relatively low propagation loss, while avoiding the lateral misalignment that may exist in similar hybrid plasmonic structures.

Acknowledgements The work at Beihang University was supported by 973 Program (2009CB930702), NSFC (61221061/61077064), National key scientific instruments and equipment development special fund management (2011YQ0301240502) and Scholarship Award for Excellent Doctoral Student granted by Ministry of Education at Beihang University.

References

[1] R. Kirchain and L. Kimerling, Nature Photon. **1**, 303–305 (2007).
[2] G. S. Wiederhecker, C. M. B. Cordeiro, F. Couny, F. Benabid, S. A. Maier, J. C. Knight, C. H. B. Cruz, and H. L. Fragnito, Nature Photon. **1**, 115–118 (2007).
[3] M. Lipson, J. Lightwave Technol. **23**, 4222–4238 (2005).
[4] V. R. Almeida, Q. F. Xu, C. A. Barrios, and M. Lipson, Opt. Lett. **29**, 1209–1211 (2004).

[5] W. L. Barnes, A. Dereux, and T. W. Ebbesen, Nature **424**, 824–830 (2003).
[6] G. Veronis and S. H. Fan, Opt. Lett. **30**, 3359–3361 (2005).
[7] V. J. Sorger, N. D. Lanzillotti-Kimura, R.-M. Ma, and X. Zhang, Nanophotonics **1**, 17–22 (2012).
[8] R. F. Oulton, V. J. Sorger, D. A. Genov, D. F. P. Pile, and X. Zhang, Nature Photon. **2**, 496–500 (2008).
[9] R. F. Oulton, V. J. Sorger, T. Zentgraf, R. M. Ma, C. Gladden, L. Dai, G. Bartal, and X. Zhang, Nature **461**, 629–632 (2009).
[10] V. J. Sorger, Z. Ye, R. F. Oulton, Y. Wang, G. Bartal, X. Yin, and X. Zhang, Nature Commun. **2**, 331 (2011).
[11] M. Z. Alam, J. Meier, J. S. Aitchison, and M. Mojahedi, Super mode propagation in low index medium, IEEE Conf. on Laser and Electro-Optics, 2007, paper JThD112.
[12] M. Wu, Z. H. Han, and V. Van, Opt. Express **18**, 11728–11736 (2010).
[13] X. Y. Zhang, A. Hu, J. Z. Wen, T. Zhang, X. J. Xue, Y. Zhou, and W. W. Duley, Opt. Express **18**, 18945–18959 (2010).
[14] H. S. Chu, E. P. Li, P. Bai, and R. Hegde, Appl. Phys. Lett. **96**, 221103 (2010).
[15] Y. S. Bian, Z. Zheng, Y. Liu, J. S. Zhu, and T. Zhou, IEEE Photon. Technol. Lett. **23**, 884–886 (2011).
[16] R. M. Ma, R. F. Oulton, V. J. Sorger, G. Bartal, and X. A. Zhang, Nature Mater. **10**, 110–113 (2010).
[17] D. X. Dai and S. L. He, Opt. Express **17**, 16646–16653 (2009).
[18] Y. S. Bian, Z. Zheng, Y. Liu, J. S. Zhu, and T. Zhou, Opt. Express **19**, 22417–22422 (2011).
[19] J. Zhang, L. Cai, W. Bai, Y. Xu, and G. Song, Opt. Lett. **36**, 2312–2314 (2011).
[20] C. C. Huang, IEEE J. Sel. Top. Quantum Electron. **18**, 1661–1668 (2012).
[21] Y. S. Bian, Z. Zheng, X. Zhao, Y. L. Su, L. Liu, J. S. Liu, J. S. Zhu, and T. Zhou, IEEE Photon. Technol. Lett. **24**, 1279–1281 (2012).
[22] D. F. P. Pile, T. Ogawa, D. K. Gramotnev, T. Okamoto, M. Haraguchi, M. Fukui, and S. Matsuo, Appl. Phys. Lett. **87**, 061106 (2005).
[23] E. Moreno, S. G. Rodrigo, S. I. Bozhevolnyi, L. Martin-Moreno, and F. J. Garcia-Vidal, Phys. Rev. Lett. **100**, 023901 (2008).

